Volume 36
Number 4
April 2021
Pages 687–858

JAAS

Journal of Analytical Atomic Spectrometry

rsc.li/jaas

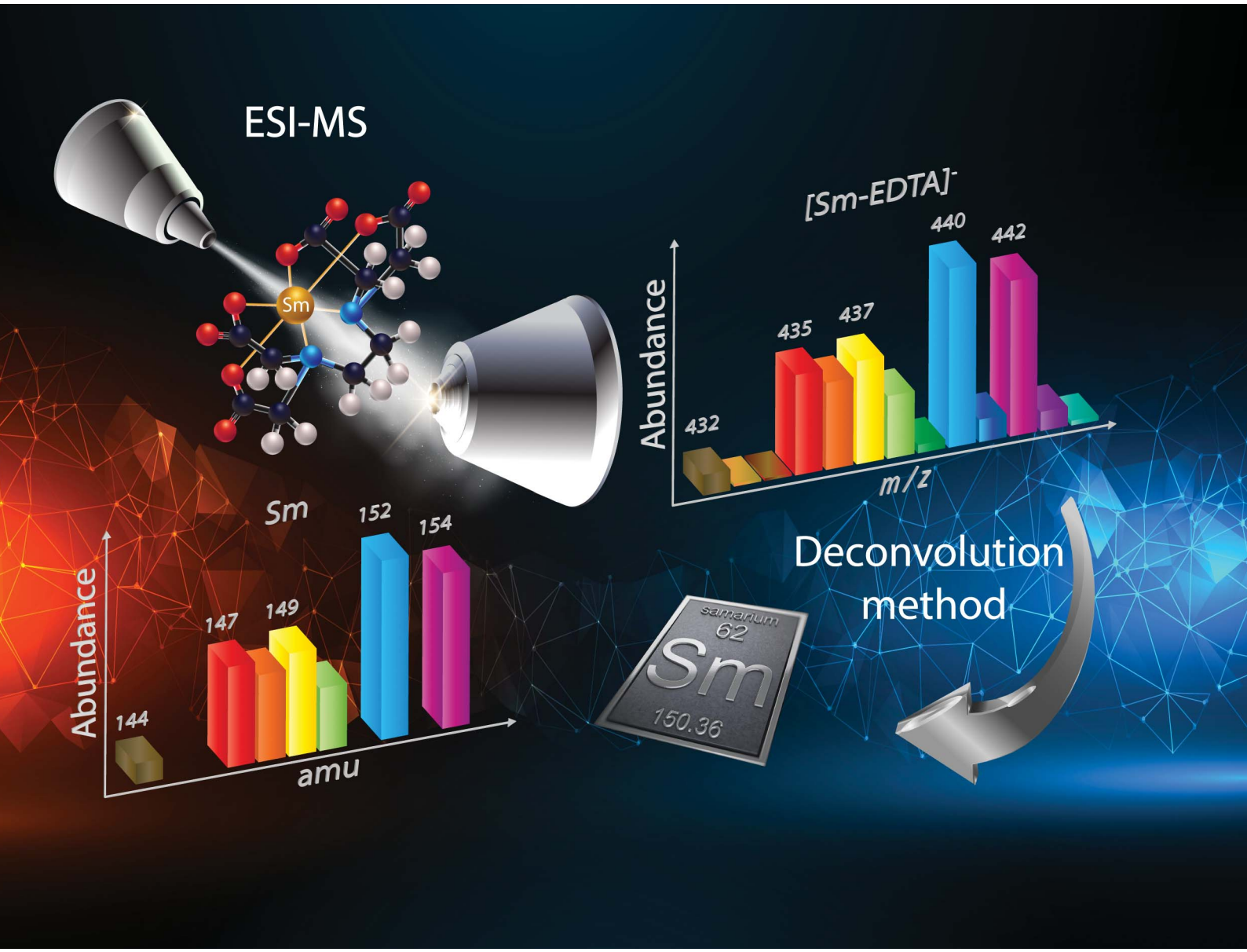

ISSN 0267-9477

ROYAL SOCIETY OF CHEMISTRY

PAPER

C. Bresson *et al.*

Determining the isotopic composition of elements from the electrospray ionization mass spectra of their chemical species

JAAS

ROYAL SOCIETY OF CHEMISTRY

PAPER

View Article Online
View Journal | View Issue

Cite this: J. Anal. At. Spectrom., 2021, 36, 758

Determining the isotopic composition of elements from the electrospray ionization mass spectra of their chemical species†

E. Blanchard,‡[ab] E. Paredes,§[a] A. Rincel,[a] A. Nonell,[a] F. Chartier[c] and C. Bresson *[a]

Electrospray ionization mass spectrometry (ESIMS) is traditionally used to analyse organic molecules, but can also be used to carry out elemental speciation studies. The challenge is here to determine the isotopic composition of elements contained in chemical species by this technique, in addition to their quantification and structural characterisation. In the present work, we determined by ESIMS the isotope ratios of samarium (Sm) and neodymium (Nd) involved in complexes containing polyaminocarboxylic acids, namely EDTA and DTPA. To this end, we developed a user-friendly deconvolution method to remove the ligand isotopic contributions from the abundance ratios measured in the ESI mass spectra of the complexes, and thus obtaining the isotopic composition of the free lanthanides. By applying the deconvolution method to EDTA complexes containing natural and enriched samarium, we obtained the ^{nat}Sm and the $^{147-149}$Sm isotopic composition directly from the mass spectra of the chemical species recorded by commercial ESI mass spectrometers, equipped with a triple quadrupole analyser (QqQ) or a linear ion trap (LIT). The isotopic composition of ^{nat}Sm and $^{147-149}$Sm were determined with a trueness better than 3.5% and 2% by ESI-QqQ-MS and better than 1% and 2% by ESI-LIT-MS, with a repeatability globally better than 3% at $k = 2$, for isotopes of relative abundances greater than 1% in samples. This method was successfully applied to determine ^{nat}Nd and ^{nat}Sm isotopic compositions from ^{nat}Nd–EDTA, ^{nat}Sm–DTPA and ^{nat}Nd–DTPA mass spectra.

Received 13th November 2020
Accepted 4th March 2021

DOI: 10.1039/d0ja00471e

rsc.li/jaas

Introduction

Speciation analysis of an element refers to the identification and structural characterisation of different chemical species in which it is contained, as well as the oxidation state identification and the quantification and isotopic characterisation of the element in each species.[1] The isotopic composition of elements incorporated in chemical species is becoming increasingly more prevalent in the field of speciation.[2] Isotope ratio variations can provide important information on the origin of the elements or on chemical, physical and biological processes in which these elements are involved. For nuclear applications, quantifying and determining the isotopic composition of radioelements have a major impact on issues such as nuclear fuel recycling or waste storage.[3] The coupling of liquid chromatography to electrospray ionization mass spectrometry (LC-ESIMS) makes it possible to structurally characterize and quantify chemical species after their separation.[4,5] However, the ability to directly determine the isotopic compositions of elements contained in species by ESIMS remains to be assessed to obtain comprehensive speciation information by this technique on its own. This study focuses on the measurement of natural and non-natural lanthanide's (Ln) isotopic composition contained in Ln–polyaminocarboxylic acid species by ESIMS. These measurements are of great interest in the field of speciation analysis of elements contained in species that can be found in nuclear applications.[6] Moreover, obtaining structural, elemental and isotopic data on chemical species in a single step is beneficial since it not only reduces costs and analysis time, but also handling and exposure times in the case of radioactive samples.

Although articles dealing with the study of metal–ligand interactions by ESIMS in solution and solid states are reported in the literature,[7–9] very few studies are to our knowledge dedicated to the determination of the isotopic composition of elements by ESIMS.[10–12] In general, these isotopic measurements were performed with prototypes or modified instruments and very often starting with inorganic metallic compounds such as nitrate or fluoride derivatives.[10–12] Pioneering studies were

[a]Université Paris-Saclay, CEA, Service d'Etudes Analytiques et de Réactivité des Surfaces, Gif-sur-Yvette, F-91191, France. E-mail: carole.bresson@cea.fr; Tel: +33 169088348

[b]Sorbonne Université, F-75005 Paris, France

[c]Université Paris-Saclay, CEA, Département de Physico-Chimie, F-91191 Gif-sur-Yvette, France

† Electronic supplementary information (ESI) available. See DOI: 10.1039/d0ja00471e

‡ Current address: Normandie Univ, UNIROUEN, Ecodiv, 76000 Rouen, France.

§ Current address: Departament de Dinàmica de la Terra i de l'Oceà, Facultat de Ciències de la Terra, Universitat de Barcelona, 08028 Barcelona, Spain.

performed in the 1990s using a modified quadrupole ICPMS (ICPMS-Q) in which the source was replaced by an electrospray ionization source.[10] Measurements performed with silver nitrate and thallium acetate led to $^{107}Ag/^{109}Ag$ and $^{205}Tl/^{203}Tl$ ratio determination. From the 2000s, ESIMS instruments with modified sources were tested for isotopic measurements. A quadrupole mass spectrometer in which the probe, the injection system and the counter electrode were modified, was used to measure boron isotope ratios, $^{10}B/^{11}B$.[11] In order to avoid hydride interferences, boron species were converted into a complex containing a monoisotopic ligand, namely BF_4^- by adding hydrofluoric acid to the sample. However, it must be noticed that this strategy induces the modification of the initial speciation of the element in the sample. The analysis of uranium (U) isotopic composition was performed with a linear ion trap mass spectrometer equipped with a homemade extractive electrospray source, suitable for the analysis of samples in complex matrices.[12] The approach involved performing tandem mass spectrometry experiments on uranyl nitrate compounds to obtain product ions, in order to determine the most accurate $^{235}U/^{238}U$ isotope ratio. At each fragmentation step, the abundance ratio of product ions containing the ^{235}U and ^{238}U isotopes was measured and compared against the theoretical $^{235}U/^{238}U$ isotope ratio. Through the MS^4 fragmentation step, the abundance ratio of $^{235}UO_7N_1H_2/^{238}UO_7N_1H_2$ could be obtained. However, even by using tandem mass spectrometry to fragment the species, the isotopic contributions of the remaining ligand atoms hampered the direct measurement of the element isotope ratios by ESIMS. Although all these studies allowed to obtain isotopic measurements with satisfying performance, the isotopic composition of the free elements was never reached directly.

In our case, the Ln isotopic pattern in the chemical species differ from the single-element isotopic composition due to the contributions of several atoms from the ligand, being EDTA or DTPA, no less than twelve hydrogen (H) atoms, ten carbon (C) atoms, two nitrogen (N) atoms and eight oxygen (O) atoms. In order to determine the Ln isotopic composition from the ESI mass spectra of the associated chemical species, our strategy was to develop a user-friendly deconvolution method to remove the H, C, N and O isotopic contributions from these spectra and thus directly determine the free lanthanide isotopic composition, without needing to perform several fragmentations of the chemical species by tandem mass spectrometry. By applying this deconvolution method, we determined the natural and the non-natural isotopic composition of Sm (^{nat}Sm and $^{147-149}Sm$) directly from the experimental mass spectra of the EDTA-containing complexes (^{nat}Sm–EDTA and $^{147-149}Sm$–EDTA) recorded by commercial QqQ and LIT ESIMS instruments. We further applied the deconvolution method to other Ln species containing Nd or DTPA, *i.e.* ^{nat}Nd–EDTA, ^{nat}Sm–DTPA and ^{nat}Nd–DTPA. In each case, the performance of the method was evaluated at each step in terms of its trueness and precision.

It must be pointed out that only some commercial instruments equipped with high resolution or ultra high resolution analysers could allow eliminating the need of deconvolution, but these instruments are only available in some laboratories dedicated to specific applications. The great advantage of the approach that we developed is that it is simply applicable for any users and for any metallic complexes, by implementing basic spreadsheets using data from the ESI mass spectra of the chemical species, obtained with low resolution mass spectrometers widely available in analytical chemistry laboratories.

Experimental section

Chemicals and samples

Ethylenediaminetetraacetic acid tetrasodium salt dihydrate (EDTA, $C_{10}H_{12}O_8N_2Na_4 \cdot 2H_2O$, purity ≥ 99.5%) and diethylenetriaminepentaacetic acid (DTPA, $C_{14}H_{23}O_{10}N_3$, purity ≥ 98%) were supplied by Sigma Aldrich (Saint Quentin Fallavier, France). Ultrapure water (resistivity 18.2 MΩ cm) was obtained from a Milli-Q water purification system (Millipore, Guyancourt, France). Acetonitrile (CH_3CN, LC-MS grade), formic acid (Normapur grade), ammonium acetate ($CH_3CO_2NH_4$, Normapur grade) and ammonia solution 25% were purchased from VWR Prolabo (Briare-le-Canal, France). HNO_3 65% (Merck Company, France) was distilled with an evapoclean system from Analab (France). This acid was used to prepare HNO_3 at 2% w/w in ultrapure water. Natural samarium (^{nat}Sm) and natural neodymium (^{nat}Nd) standard solutions at 1000 μg mL^{-1} in HNO_3 2% w/w were provided by Spex Certiprep Group (Longjumeau, France). The isotopic compositions of ^{nat}Sm and ^{nat}Nd

Table 1 Reference Sm and Nd isotope ratios obtained by TIMS and associated relative abundances in ^{nat}Sm,[13] $^{147-149}Sm$ [14] and ^{nat}Nd;[13] the values between brackets correspond to the expanded uncertainty ($k = 2$). The ^{nat}Sm and ^{nat}Nd isotope ratios were internally normalized to $^{147}Sm/^{149}Sm = 1.08680(32)$ and to $^{146}Nd/^{144}Nd = 0.72333(16)$. The uncertainty of the relative abundance of ^{nat}Sm, $^{147-149}Sm$ and ^{nat}Nd isotopes was calculated with the Kragten method[15]

	Isotope ratio	Measured	Isotope	Relative abundance (%)
^{nat}Sm	$^{144}Sm/^{150}Sm$	0.41943(59)	^{144}Sm	3.096(4)
	$^{147}Sm/^{150}Sm$	2.0365(13)	^{147}Sm	15.034(5)
	$^{148}Sm/^{150}Sm$	1.52568(87)	^{148}Sm	11.263(3)
	$^{149}Sm/^{150}Sm$	1.8739(10)	^{149}Sm	13.833(3)
	$^{152}Sm/^{150}Sm$	3.6173(23)	^{150}Sm	7.382(4)
	$^{154}Sm/^{150}Sm$	3.0733(21)	^{152}Sm	26.704(8)
			^{154}Sm	22.688(8)
$^{147-149}Sm$	$^{144}Sm/^{147}Sm$	0.00094(4)	^{144}Sm	0.047(2)
	$^{148}Sm/^{147}Sm$	0.05343(31)	^{147}Sm	50.005(51)
	$^{149}Sm/^{147}Sm$	0.9035(18)	^{148}Sm	2.672(15)
	$^{150}Sm/^{147}Sm$	0.02526(8)	^{149}Sm	45.178(46)
	$^{152}Sm/^{147}Sm$	0.01133(4)	^{150}Sm	1.263(3)
	$^{154}Sm/^{147}Sm$	0.00536(3)	^{152}Sm	0.567(2)
			^{154}Sm	0.268(1)
^{nat}Nd	$^{142}Nd/^{144}Nd$	1.13966(28)	^{142}Nd	27.109(6)
	$^{143}Nd/^{144}Nd$	0.51097(10)	^{143}Nd	12.155(3)
	$^{145}Nd/^{144}Nd$	0.34874(4)	^{144}Nd	23.787(3)
	$^{146}Nd/^{144}Nd$	0.72333	^{145}Nd	8.296(2)
	$^{148}Nd/^{144}Nd$	0.24302(20)	^{146}Nd	17.206(4)
	$^{150}Nd/^{144}Nd$	0.23821(14)	^{148}Nd	5.781(5)
			^{150}Nd	5.666(4)

Table 2 Setting parameters selected for the experiments

	ESI-QqQ-MS TSQ quantum	ESI-LIT-MS LTQ Velos Pro
Spray voltage	−3.7 kV	
Capillary transfer temperature (°C)	280	
Vaporisation temperature (°C)	90	
Sheath gas (a.u.)	10	
Auxiliary gas (a.u.)	10	5
Skimmer offset (V)	0	—
S-lens (%)	—	70
Fragmentation in source (eV)	—	40
Scan number	100	
Scan time (s)	0.7	—
FWHM/Scan rate (kDa s^{-1})	0.5/-	0.35/10

were determined by thermal ionization mass spectrometry (TIMS) (VG 354, VG Elemental); this data is provided in Table 1.[13] A double spike $^{147-149}$Sm solution was prepared beforehand by dissolution in nitric acid of two Sm_2O_3 powders, enriched in ^{147}Sm (94.40%) and in ^{149}Sm (95.13%), to obtain a ^{147}Sm/^{149}Sm isotope ratio close to one.[14] The concentration of HNO_3 in this enriched stock solution was around 4.8 mol L^{-1} and the total Sm concentration of 9.75×10^{-4} mol L^{-1} (144.3 μg mL^{-1}). The isotopic composition of the double spike was characterized by TIMS (Isoprobe-T mass spectrometer, IsotopX Ltd) and is given in Table 1.[14]

Two stock solutions of EDTA were prepared at 5×10^{-3} mol L^{-1} and 1.76×10^{-3} mol L^{-1} and a stock solution of DTPA was also prepared at 5×10^{-3} mol L^{-1} by dissolution of the corresponding powder in ultrapure water.

A 5×10^{-3} mol L^{-1} (751.8 μg mL^{-1}) ^{nat}Sm stock solution was prepared by dilution of the ^{nat}Sm standard solution in ultrapure water. This stock solution was mixed with the 5×10^{-3} mol L^{-1} EDTA stock solution to obtain a Sm : EDTA ratio of 1 : 1.2, with $[^{nat}Sm] = 2.27 \times 10^{-3}$ mol L^{-1}. This solution was used to develop the deconvolution method.

A 8.34×10^{-4} mol L^{-1} (125.5 μg mL^{-1}) ^{nat}Sm stock solution was prepared by dilution of the ^{nat}Sm standard solution in a 4.8 mol L^{-1} HNO_3 solution. The two ^{nat}Sm and $^{147-149}$Sm stock solutions were evaporated and then redissolved in HNO_3 (2% w/w) to obtain a total Sm concentration of 5×10^{-3} mol L^{-1} (751.8 μg mL^{-1}) for ^{nat}Sm and 5.85×10^{-3} mol L^{-1} (866 μg mL^{-1}) for $^{147-149}$Sm. Then both solutions were mixed with the 1.76×10^{-3} mol L^{-1} EDTA stock solution to obtain a ^{nat}Sm : EDTA ratio of 1 : 1.2, with $[^{nat}Sm] = 1.1 \times 10^{-3}$ mol L^{-1} and a $^{147-149}$Sm : EDTA ratio of 1 : 1, with $[^{147-149}Sm] = 1.3 \times 10^{-3}$ mol L^{-1}. These two solutions were used to validate the deconvolution method.

In the same manner, a 5×10^{-3} mol L^{-1} (721.2 μg mL^{-1}) ^{nat}Nd stock solution was prepared by dilution of the corresponding standard solution in ultrapure water. An appropriate volume of ^{nat}Ln (Ln = Nd or Sm) stock solutions were mixed with stock solution of EDTA or DTPA to obtain an Ln–polyaminocarboxylic acid ratio of 1 : 1.2, with $[^{nat}Ln] = 2.27 \times$

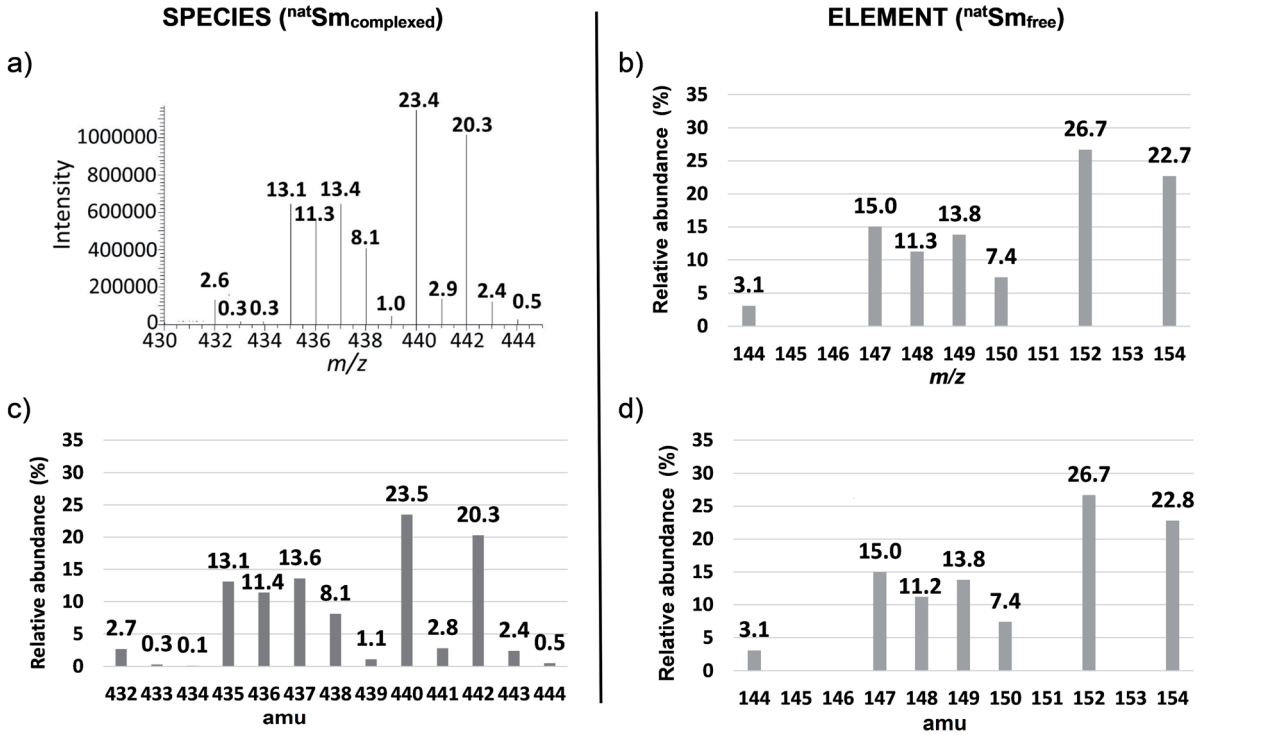

Fig. 1 Isotopic patterns of ^{nat}Sm–EDTA and ^{nat}Sm (a) experimental mass spectrum of ^{nat}Sm–EDTA recorded by ESI-LIT-MS in full scan mode, (b) reference ^{nat}Sm isotopic pattern obtained by TIMS,[13] (c) ^{nat}Sm–EDTA isotopic pattern calculated with the Yergey convolution method[17] (d) ^{nat}Sm isotopic pattern obtained by deconvolution of the experimental ESI mass spectrum of ^{nat}Sm–EDTA.

Carbon

Number of ^{12}C	Number of ^{13}C	*m/z*	Abundance	Abundance (ppm)
10	0	120	0.898	898008
9	1	121	0.097	97126
8	2	122	0.005	4727
7	3	123	1.10^{-4}	136
6	4	124	3.10^{-6}	3
5	5	125	3.10^{-8}	3.10^{-2}

Hydrogen

Number of ^{1}H	Number of ^{2}H	*m/z*	Abundance	Abundance (ppm)
12	0	12	0.999	998621
11	1	13	0.001	1378
10	2	14	9.10^{-7}	0.9

Fig. 2 Atomic abundance of carbon and hydrogen isotopic permutations for deprotonated EDTA ($C_{10}H_{12}N_2O_8$).

10^{-3} mol L^{-1}. These solutions were used to apply the deconvolution method to ^{nat}Nd–EDTA, ^{nat}Sm–DTPA and ^{nat}Nd–DTPA species.

In all cases, the pH of these solutions was adjusted to 3.2 by adding a 25% ammonia solution, in order to obtain common pH in the aqueous back-extraction phases of spent nuclear fuel treatment processes. In view of the future coupling of chromatography to ESIMS, the working samples were prepared by diluting the previous solutions in a mobile phase made of 70/30 (v/v) acetonitrile/water, 0.5% formic acid and 15×10^{-3} mol L^{-1} of ammonium acetate, to reach a final Ln concentration of 10^{-4} mol L^{-1} (15 μg mL^{-1} for Sm and 14.5 μg mL^{-1} for Nd).

ESIMS instrumentation

We used a TSQ quantum quadrupole mass spectrometer (ESI-QqQ-MS, Thermo Fisher Scientific, USA) equipped with an H-ESI-II ionization source and a triple quadrupole analyser. We also used a LTQ Velos Pro mass spectrometer (ESI-LIT-MS, Thermo Fisher Scientific, USA) equipped with an H-ESI-II ionization source and a linear ion trap analyser. The samples were continuously injected into the spectrometers at a flow rate of 10 μL min^{-1}. All ESIMS spectra were recorded in negative ionization mode and in MS mode.

For both instruments, the acquisition parameters leading to the best performance for ^{nat}Sm–EDTA complex were selected (Table 2).

These parameters were also applied for abundance ratio measurements in $^{147-149}$Sm–EDTA, ^{nat}Nd–EDTA, ^{nat}Sm–DTPA and ^{nat}Nd–DTPA. With the ESI-QqQ-MS and the ESI-LIT-MS, the abundance ratios of complexed lanthanides were determined based on the average of ten measurements for all samples containing lanthanides with natural isotopic composition and on the average of three series of ten measurements for the sample containing samarium with non-natural isotopic composition.

A ^{nat}Sm–EDTA solution was used as the control standard at the beginning and end of the analytical sessions to measure $^{147-149}$Sm–EDTA abundance ratios, in order to correct potential instrumental mass bias values. This standard was prepared in

Table 3 Relative abundances (in %) for each *m/z* ratio in ^{nat}Sm–EDTA calculated with the Yergey convolution method[17] using the relative isotopic abundances of H, C, N and O from IUPAC[18] and from TIMS data for ^{nat}Sm[13]

Species																				
Element	432	433	434	435	436	437	438	439	440	441	442	443	444	445	446	447	448	449	450	451
^{144}Sm	2.7×10^{-2}	3×10^{-2}	1×10^{-3}	5.9×10^{-5}	6.2×10^{-6}	4.7×10^{-7}	2.1×10^{-8}	6.4×10^{-10}	4.6×10^{-12}	1.2×10^{-14}	8.9×10^{-18}									
^{147}Sm				0.3131	1.6×10^{-2}	0.003	2.9×10^{-4}	3.0×10^{-5}	2.3×10^{-6}	1.0×10^{-7}	3.1×10^{-9}	2.2×10^{-11}	5.7×10^{-14}	4.3×10^{-17}						
^{148}Sm					9.8×10^{-2}	1.2×10^{-2}	2×10^{-3}	2.1×10^{-4}	2.2×10^{-5}	1.7×10^{-6}	7.6×10^{-8}	2.3×10^{-9}	1.7×10^{-11}	4.3×10^{-14}	3.3×10^{-17}					
^{149}Sm						0.121	1.4×10^{-2}	3×10^{-3}	2.6×10^{-4}	2.8×10^{-5}	2.1×10^{-6}	9.3×10^{-8}	2.1×10^{-9}	2.1×10^{-11}	5.2×10^{-14}	4.0×10^{-17}				
^{150}Sm							0.064	8×10^{-3}	1×10^{-3}	1.4×10^{-4}	1.5×10^{-5}	1.1×10^{-6}	5.0×10^{-8}	1.5×10^{-9}	1.1×10^{-11}	2.8×10^{-14}	2.1×10^{-17}			
^{152}Sm									0.233	2.8×10^{-2}	5×10^{-2}	1×10^{-3}	5.3×10^{-5}	4.1×10^{-6}	1.8×10^{-7}	5.5×10^{-69}	4.0×10^{-11}	1.0×10^{-13}	7.7×10^{-17}	
^{154}Sm											0.198	2.4×10^{-2}	5×10^{-3}	4.3×10^{-4}	4.5×10^{-5}	3.4×10^{-6}	1.5×10^{-7}	4.7×10^{-9}	3.4×10^{-11}	8.6×10^{-14}
Total	0.03	0.00	0.00	0.13	0.11	0.14	0.08	0.01	0.23	0.03	0.20	0.02	0.00	0.00	0.00	0.00	0.00	0.00	0.00	0.00
Abundance (%)	2.7	0.3	0.1	13.1	11.4	13.6	8.1	1.1	23.5	2.8	20.3	2.4	0.5	0.0	0.0	0.0	0.0	0.0	0.0	0.0

the same manner as the enriched $^{147-149}$Sm–EDTA sample, by respecting the initial composition of the matrix (HNO_3 4.8 mol L^{-1}). No instrumental mass bias was observed during these measurement sessions but background signal variations were observed in the control standard. These background signal variations were corrected on the enriched sample by normalizing and subtracting them from the intensities measured on the control standard.

Results and discussion

Development of the deconvolution method

This method was developed with ^{nat}Sm–EDTA and further applied to the other Ln complexes. Briefly, we first calculated the theoretical isotopic pattern of ^{nat}Sm–EDTA by convolution. Based on this initial convolution data, we then defined the matrix of the isotopic contributions of the ligand atoms H, C, N and O. By combining this latter matrix with the measured intensities in the mass spectra of ^{nat}Sm–EDTA, we established a system of equations to determine the ^{nat}Sm isotopic composition. Among the available convolution methods,[16] we used the readily implemented Yergey's polynomial method[17] taking into account the stoichiometry of the complex and the relative isotopic abundances using both International Union of Pure and Applied Chemistry (IUPAC) data for H, C, N and O[18] and TIMS data measured at the laboratory for ^{nat}Sm[13] (Table 1 and Fig. 1b). By applying the Yergey's convolution method, we calculated the theoretical mass spectrum of negatively monocharged ^{nat}Sm–EDTA (Fig. 1c).

Except for Sm for which the stoichiometry is one, we calculated the atomic abundance of each isotopic permutation for each element using eqn (1):

$$A = \frac{n!}{a!b!c!\ldots} r_1{}^a r_1{}^b r_1{}^c \ldots \quad (1)$$

where A: atomic abundance for each permutation, n: number of atoms of the element, a, b, c, *etc*: number of isotopes of the element in the permutation, $r_1 r_2 r_3$,*etc.*: atomic abundance of each isotope of the element.

For example, one of the permutations of C_{10} is $^{12}C_8{}^{13}C_2$, leading to the atomic abundance of 4727 ppm (Fig. 2):

$$A_{^{12}C_8{}^{13}C_2} = \frac{10!}{8!2!} \times 0.9893^8 \times 0.0107^2 = 4.727 \times 10^{-3}$$

We disregarded all permutations with abundances lower than 10 ppm for the next step of our study as they have a negligible impact on our calculations.

In a second step, the abundance of each permutation for ^{nat}Sm–EDTA was determined. It corresponds to the product of the abundance of the isotopic permutations of each element, calculated in the first step, by respecting the stoichiometry of the species. For example, the abundance of the $^{148}Sm^{12}C_8{}^{13}C_2{}^{1}H_{12}{}^{14}N_2{}^{16}O_7{}^{18}O_1$ permutation at m/z 440 was calculated according to eqn (2), resulting in 8.51×10^{-6}:

$$A_{^{148}Sm^{12}C8^{13}C2^{1}H12^{14}N2^{16}O7^{18}O1} = A_{^{148}Sm} \times A_{^{12}C8^{13}C2} \times A_{^{1}H12} \times A_{^{14}N2} \times A_{^{16}O7^{18}O1} \quad (2)$$

The third step consisted in summing the combined abundances of all the previous calculated permutations for each m/z ratio and Sm isotope. Table 3 gives the results in matrix form, with the m/z ratios of the ^{nat}Sm–EDTA in columns and the ^{nat}Sm isotopes in rows.

By way of example, in the cell corresponding to m/z 440 and ^{148}Sm, the abundances of all the permutations corresponding to this m/z with ^{148}Sm (*e.g.* $A_{^{148}Sm^{12}C_8{}^{13}C_2{}^{1}H_{12}{}^{14}N_2{}^{16}O_7{}^{18}O_1}$ and $A_{^{148}Sm^{12}C_9{}^{13}C_1{}^{1}H_{12}{}^{14}N_1{}^{15}N_1{}^{16}O_7{}^{18}O_1}$) were summed. The theoretical relative abundance for each m/z ratio of ^{nat}Sm–EDTA was then calculated by summing the values of each column. On the basis of these calculated abundances, the resulting theoretical ^{nat}Sm–EDTA isotopic pattern appears to be consistent with the experimental mass spectrum, as illustrated in Fig. 1a and c.

By considering the range of natural abundance variations provided by IUPAC for H, C, N and O,[19] the maximum impact on calculated abundance ratios was ±1.4% for the ^{nat}Sm–EDTA ratio of 432/438, with the species at m/z = 432 containing the less abundant ^{144}Sm isotope (3.1%). The difference was lower than 0.1% for the other isotope ratios. These variations were therefore considered to be negligible in this study. That being said, the theoretical bias, corresponding to the difference between experimental ^{nat}Sm–EDTA abundance ratios and calculated ^{nat}Sm–EDTA abundances ratios by convolution, was calculated for all abundance ratios of ^{nat}Sm–EDTA. This theoretical bias was better than 3% with repeatability of 3% for results obtained by ESI-QqQ-MS, and better than 1% with repeatability of 1% with the ESI-LIT-MS (data not shown). To determine the ^{nat}Sm isotopic composition by deconvolution of the experimental ^{nat}Sm–EDTA mass spectra obtained by ESIMS, the next step was to remove the isotopic contributions of H, C, N

Table 4 H, C, N and O isotopic contribution matrix in the isotopic pattern of ^{nat}Sm–EDTA

H, C, N and O isotopic contributions	m/z ratio						
	432	435	436	437	438	440	442
^{144}Sm	0.873	1.907×10^{-3}	1.989×10^{-4}	1.518×10^{-5}	6.713×10^{-7}	1.493×10^{-10}	2.887×10^{-16}
^{147}Sm		0.873	0.105	2.0×10^{-2}	1.907×10^{-3}	1.518×10^{-5}	2.077×10^{-8}
^{148}Sm			0.873	0.105	2.0×10^{-2}	1.989×10^{-4}	6.712×10^{-7}
^{149}Sm				0.873	0.105	1.907×10^{-3}	1.518×10^{-5}
^{150}Sm					0.873	2.0×10^{-2}	1.989×10^{-4}
^{152}Sm						0.873	2.0×10^{-2}
^{154}Sm							0.873

and O at each m/z ratio. For this, a system of n equations with n unknowns, was defined from the abundance matrix (Table 3) and further solved. In the case of ^{nat}Sm–EDTA, n is equal to 7, which represents the atomic abundances of the seven ^{nat}Sm isotopes. The H, C, N and O contributions for each m/z ratio were calculated by dividing each row of the matrix by the atomic abundance of corresponding ^{nat}Sm isotopes. A new matrix including only the H, C, N and O isotopic contributions from EDTA was then obtained (Table 4).

The ^{nat}Sm isotope ratios were then determined from the measured intensities (I) of the ^{nat}Sm–EDTA isotopic pattern and the contribution matrix of the H, C, N, O isotopes at each m/z ratio, by defining a system of 7 equations, with the 7 unknowns being the atomic abundances of ^{nat}Sm isotopes.

For example, for m/z 432 and m/z 435 (Table 4 and eqn (3)):

$$^{432}\mathrm{I} = 0.873 \times {}^{144}\mathrm{A} \text{ and } {}^{435}\mathrm{I} = 1.907 \times 10^{-3} \times {}^{144}\mathrm{A} + 0.873 \times {}^{147}\mathrm{A} \quad (3)$$

The ^{nat}Sm isotope ratios were then determined by combining the obtained atomic abundances. An example is given below for the ^{147}Sm/^{144}Sm ratio (eqn (4)):

$$\underbrace{\left[\frac{^{432}\mathrm{I}}{^{435}\mathrm{I}} = \frac{0.873 \times {}^{144}\mathrm{A}}{1.907 \times 10^{-3} \times {}^{144}\mathrm{A} + 0.873 \times {}^{147}\mathrm{A}}\right]}_{\text{INTENSITIES MEASURED}} \longrightarrow \underbrace{\left[\frac{^{147}\mathrm{A}}{^{144}\mathrm{A}} = \frac{0.873 - 1.907 \times 10^{-3} \times \frac{^{432}\mathrm{I}}{^{435}\mathrm{I}}}{0.873 \times \frac{^{432}\mathrm{I}}{^{435}\mathrm{I}}}\right]}_{\text{ISOTOPE RATIO}} \quad (4)$$

$$\text{SPECIES} \qquad\qquad \text{ELEMENT}$$

Since the deconvolution method developed does not depend on the Sm isotopic composition, it is particularly relevant for any applications in which non-natural isotopic abundances are involved.

Determination of isotopic composition of lanthanides contained in chemical species by ESIMS

The experimental mass spectra of ^{nat}Sm–EDTA (Fig. 1a) were deconvoluted to obtain the isotopic pattern of ^{nat}Sm (Fig. 1d). The results are given in Table 5, together with the reference isotope ratios of ^{nat}Sm, the trueness, calculated as the difference between experimental ^{nat}Sm isotope ratios obtained after deconvolution and the reference ^{nat}Sm isotope ratios, as well as the repeatability of the measurements.

The bias before deconvolution, calculated as the difference between the experimental ^{nat}Sm–EDTA abundance ratios and the reference ^{nat}Sm isotope ratios, ranged between 8 and 24%. After deconvolution, the ^{nat}Sm isotope ratios were determined with a trueness better than 3.5% and a repeatability of about 3% for ESI-QqQ-MS, and a trueness better than 1.0% and a repeatability of about 1% for ESI-LIT-MS.

The same approach was applied to a double spike enriched in $^{147-149}$Sm of known isotopic composition and complexed with EDTA. The isotopic composition of $^{147-149}$Sm was then determined from the $^{147-149}$Sm–EDTA mass spectra recorded with ESI-QqQ-MS and ESI-LIT-MS.

This double spike was selected since $^{147-149}$Sm–EDTA leads to a more complex spectrum than ^{nat}Sm–EDTA for the less abundant Sm isotopes (Fig. 1a and 3a).

In particular, the less abundant Sm isotope of ^{nat}Sm (^{144}Sm) led to 2.7% abundance at m/z 432 in the ^{nat}Sm–EDTA convoluted spectrum (Fig. 1c). This mass was not impacted by the H, C, N and O isotopic contributions because it is associated with the lightest Sm isotope. The abundances in the ^{nat}Sm–EDTA spectrum ranging between 8.1 and 23.5% (Fig. 1c) are associated with Sm isotopes with abundances ranging between 7.4 and 26.7% (Fig. 1b). Conversely, there are two major ions with abundances of 43.7 and 40.7% at m/z 435 and m/z 437 in the $^{147-149}$Sm–EDTA convoluted spectrum (Fig. 3c). These peaks are related to ^{147}Sm and ^{149}Sm isotopes with abundances of 50.0 and 45.2% (Fig. 3b). The other Sm isotopes showed much lower abundances (less than 2.7%) and were all significantly impacted by the H, C, N and O isotopic contributions. In particular, the relative abundances of ^{148}Sm and ^{150}Sm were 2.7% and 1.3%

Table 5 ^{nat}Sm isotope ratios determined after deconvolution of ^{nat}Sm–EDTA mass spectra acquired with ESI-QqQ-MS and ESI-LIT-MS. The measured ratios were determined based on the average of ten measurements. Trueness after deconvolution was calculated in comparison with the reference ^{nat}Sm isotope ratios obtained by TIMS.[13] Repeatability was expressed at $k = 2$ after deconvolution

^{nat}Sm isotope ratios		^{144}Sm/^{150}Sm	^{147}Sm/^{150}Sm	^{148}Sm/^{150}Sm	^{149}Sm/^{150}Sm	^{152}Sm/^{150}Sm	^{154}Sm/^{150}Sm
TIMS reference value[13]		0.4194	2.0365	1.5257	1.8739	3.6173	3.0733
ESI-QqQ-MS	Average ($n = 10$)	0.4062	1.9799	1.4976	1.8502	3.6264	3.0474
	Trueness (%)	**−3.1**	**−2.8**	**−1.8**	**−1.3**	**0.3**	**−0.8**
	Repeatability (%)	2.2	1.2	2.8	2.0	1.5	1.9
ESI-LIT-MS	Average ($n = 10$)	0.4166	2.0376	1.5296	1.8718	3.6216	3.0860
	Trueness (%)	**−0.7**	**0.1**	**0.3**	**−0.1**	**0.1**	**0.4**
	Repeatability (%)	1.0	0.9	0.7	0.9	0.7	0.7

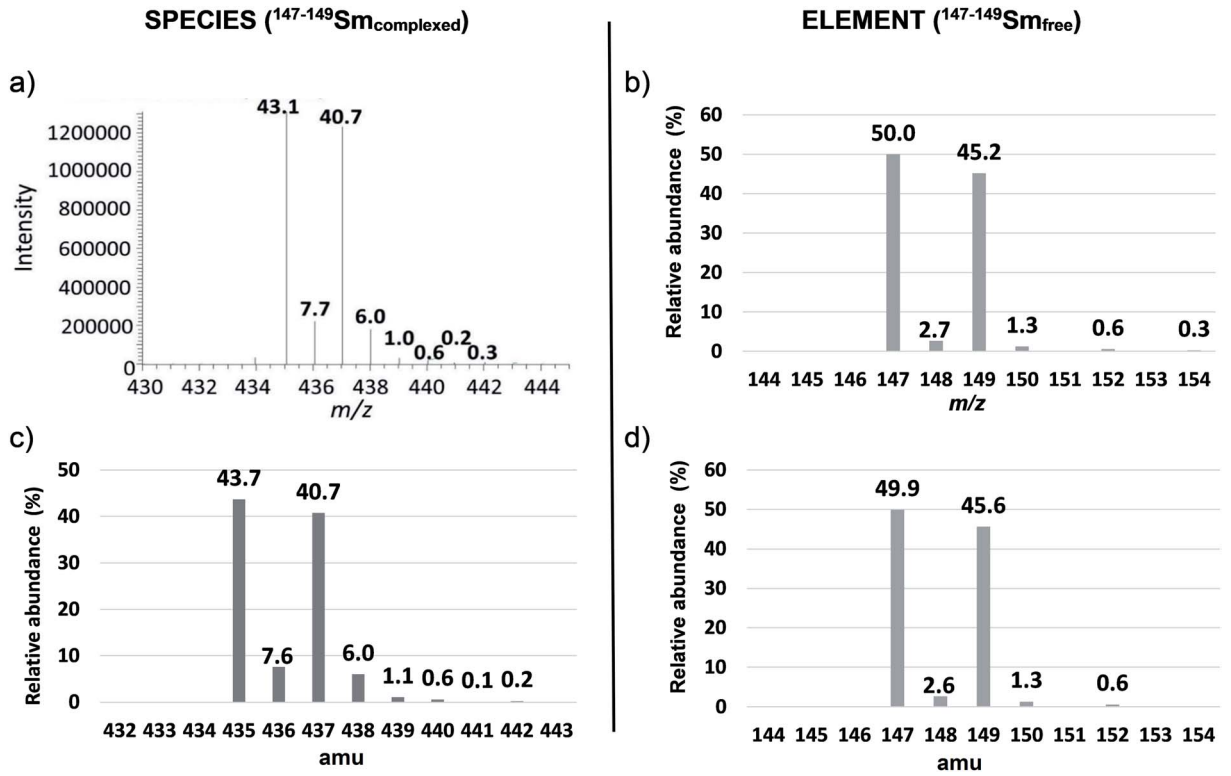

Fig. 3 Isotopic patterns of $^{147-149}$Sm–EDTA and $^{147-149}$Sm (a) experimental mass spectrum of $^{147-149}$Sm–EDTA recorded by ESI-LIT-MS in full scan mode, (b) reference $^{147-149}$Sm isotopic pattern obtained by TIMS,[14] (c) $^{147-149}$Sm–EDTA isotopic pattern calculated with the Yergey convolution method,[17] (d) $^{147-149}$Sm isotopic pattern obtained by deconvolution of the experimental ESI mass spectrum of $^{147-149}$Sm–EDTA.

(Fig. 3b), and 7.6% and 6% respectively for m/z 436 and m/z 438 in the $^{147-149}$Sm–EDTA isotopic pattern (Fig. 3c).

As the theoretical bias calculated with m/z 435 as reference was systematically positive with ESI-LIT-MS for the ^{148}Sm–EDTA/^{147}Sm–EDTA ratio and for all abundance ratios of $^{147-149}$Sm–EDTA with ESI-QqQ-MS (data not shown), we attributed these interferences to the residual nitrates coming from the sample preparation. To remove such interference, corrections detailed in the experimental part were applied. After correction, the theoretical bias and the repeatability at $k = 2$ were better than 2% and 4% with ESI-QqQ-MS (data not shown), for all abundance ratios for which Sm isotope abundances were greater than 1%. With ESI-LIT-MS, the theoretical bias and the repeatability were better than 2% for all abundance ratios, except for the ^{152}Sm–EDTA/^{147}Sm–EDTA ratio, for which the theoretical bias was about 9%, because of the too low intensity of the signal. The experimental ESI-LIT-MS mass spectra of $^{147-149}$Sm–EDTA (Fig. 3a) were deconvoluted to obtain the $^{147-149}$Sm isotopic composition (Fig. 3d). Table 6 gives the isotope ratios of $^{147-149}$Sm determined after deconvolution of mass spectra, the reference $^{147-149}$Sm isotope ratios, the trueness and the repeatability of the measurements.

The bias before deconvolution for the major ^{149}Sm–EDTA/^{147}Sm–EDTA abundance ratio was around 4% with the two ESI instruments, whereas it was between 25% and 450% for the minor abundance ratios. After deconvolution, we achieved a trueness better than 2% with the two instruments, except for the ^{152}Sm/^{147}Sm ratio for which the ^{152}Sm abundance was 0.6%

Table 6 $^{147-149}$Sm isotope ratios determined after deconvolution of $^{147-149}$Sm–EDTA mass spectra acquired with ESI-QqQ-MS and ESI-LIT-MS. The measured ratios were based on the average of three replicates of ten measurements. Trueness after deconvolution was calculated in comparison with the reference $^{147-149}$Sm isotope ratios obtained by TIMS.[14] Repeatability is expressed at $k = 2$ after deconvolution

$^{147-149}$Sm isotope ratios		^{148}Sm/^{147}Sm	^{149}Sm/^{147}Sm	^{150}Sm/^{147}Sm	^{152}Sm/^{147}Sm
TIMS reference value[14]		0.0534	0.9035	0.0253	0.0113
ESI-QqQ-MS	Average ($n = 3 \times 10$)	0.0531	0.9135	0.0258	0.0061
	Trueness (%)	**−0.6**	**1.1**	**2.0**	**−46.3**
	Repeatability (%)	9.3	3.0	12.9	7.5
ESI-LIT-MS	Average ($n = 3 \times 10$)	0.0524	0.9136	0.0253	0.0125
	Trueness (%)	**−2.0**	**1.1**	**0.3**	**10.4**
	Repeatability (%)	1.8	0.2	2.5	2.1

Table 7 ^{nat}Nd isotope ratios determined after deconvolution of ^{nat}Nd–DTPA mass spectra acquired with ESI-QqQ-MS and ESI-LIT-MS. The measured ratios were based on the average of ten measurements. Trueness after deconvolution was calculated in comparison with the reference ^{nat}Nd isotope ratios obtained by TIMS.[13] Repeatability was expressed at $k = 2$ after deconvolution

^{nat}Nd isotope ratios		^{142}Nd/^{144}Nd	^{143}Nd/^{144}Nd	^{145}Nd/^{144}Nd	^{146}Nd/^{144}Nd	^{148}Nd/^{144}Nd	^{150}Nd/^{144}Nd
TIMS reference value[13]		1.1397	0.5110	0.3487	0.7233	0.2430	0.2382
ESI-QqQ-MS	Average ($n = 10$)	1.1304	0.5090	0.3479	0.7205	0.2444	0.2391
	Trueness (%)	**−0.8**	**−0.4**	**−0.2**	**−0.4**	**0.6**	**0.4**
	Repeatability (%)	2.1	2.1	2.1	1.4	2.1	2.4
ESI-LIT-MS	Average ($n = 10$)	1.1225	0.5089	0.3451	0.7228	0.2432	0.2366
	Trueness (%)	**−1.5**	**−0.4**	**−1.0**	**−0.1**	**0.1**	**−0.7**
	Repeatability (%)	0.3	0.4	0.5	0.3	0.3	0.4

(Fig. 3d). For this ratio, trueness was worse than 10%. With ESI-QqQ-MS, the repeatability was 3% for the major ^{149}Sm/^{147}Sm ratio, while it was about 10% for the other ratios. With ESI-LIT-MS, the repeatability was better than 2.5% for all isotope ratios. These results confirm the validity of all the isotopic measurements we performed with commercial ESIMS instruments as well as the readily implementable deconvolution method, for isotopes of relative abundances greater than 1% in samples. The $^{147–149}$Sm isotope ratios were determined by ESI-QqQ-MS and ESI-LIT-MS with a trueness better than 3% for Sm isotope ratios ranging between 0.025 and 0.9 with isotope abundances as low as 1.3%. This is true despite the strong impact of the H, C, N and O isotopic contributions from adjacent major peaks 20 to 40 times more intense.

We further carried out isotopic measurements starting with ESI mass spectra of chemical species containing another lanthanide (^{nat}Nd–EDTA), another ligand (^{nat}Sm–DTPA) and different lanthanide and ligand (^{nat}Nd–DTPA). The isotope ratios of ^{nat}Nd and ^{nat}Sm were then determined by applying the deconvolution method to the associated lanthanide complexes and compared to reference ratios of the free lanthanides. The isotope ratios of ^{nat}Nd determined after deconvolution of ^{nat}Nd–DTPA mass spectra (Fig. S1†), the reference ^{nat}Nd isotope ratios, the trueness and the repeatability of the measurements are given in Table 7, while the results obtained for ^{nat}Nd–EDTA and ^{nat}Sm–DTPA are provided in Tables S1 and S2, as well as in Fig. S2 and S3.†

For all abundance ratios of ^{nat}Nd–DTPA measured by ESI-QqQ-MS and ESI-LIT-MS, a bias between 0 and 30% was obtained before deconvolution in comparison with reference ^{nat}Nd isotope ratios obtained by TIMS.[13] After deconvolution of the ^{nat}Nd–DTPA mass spectra, the ^{nat}Nd isotope ratios were determined with a trueness better than 1% and a repeatability of around 2% with ESI-QqQ-MS, and a trueness better than 1.5% and a repeatability of around 0.5% with ESI-LIT-MS (Table 7).

These results indicate that the performance of ^{nat}Nd isotope ratio measurements obtained from ESI mass spectra of ^{nat}Nd–DTPA are very good and similar to those measured for the ^{nat}Sm–EDTA species, by retaining the same experimental parameters.

By deconvolution of the mass spectra of ^{nat}Nd–EDTA and ^{nat}Sm–DTPA, the isotope ratios of the ^{nat}Ln were determined with a trueness better than 3.0% and a repeatability of around 2.5% with ESI-QqQ-MS, and a trueness better than 2.5% and a repeatability of around 0.5% with ESI-LIT-MS (Tables S1, S2, Fig. S2 and S3†). Overall, we were able to demonstrate that the substitution of Sm by Nd in the EDTA or DTPA chemical species has no impact either on the quality of the isotopic measurements with the two ESIMS instruments, or on the performance of the deconvolution method that we developed.

This work was carried out using model samples but can be performed with more complex samples, by coupling a separation step to ESIMS, to isolate the chemical species and the potential interferents before the analysis step.

Conclusion

The aim of the present work was to determine the isotopic composition of elements contained in chemical species, by electrospray mass spectrometry. In particular, the isotopic composition of natural and non-natural Sm and natural Nd contained in EDTA and DTPA complexes, were determined using two different mass spectrometers. To meet this aim, we developed a user-friendly deconvolution method to directly determine the Ln isotopic composition based on ESI mass spectra of the associated chemical species, by removing the isotopic contributions of the atoms from the ligand without performing fragmentations experiments by tandem mass spectrometry. By applying the deconvolution method to the mass spectra of Sm–EDTA species containing natural and enriched samarium, a trueness and a repeatability globally better than 3% were obtained for all isotope ratios of Sm with isotope abundances greater than 1%, using ESI-QqQ-MS and ESI-LIT-MS. The performance of the $^{147–149}$Sm–EDTA abundance ratio measurements and deconvolution method demonstrated the approach applicability for non-natural sample analysis; including low-abundance isotopes strongly impacted by H, C, N, and O isotopic contributions from the major neighbouring isotopes. The deconvolution method was also successfully applied to other Ln–polyaminocarboxylic species such as ^{nat}Nd–EDTA, ^{nat}Sm–DTPA and ^{nat}Nd–DTPA, leading to similar performance of trueness and repeatability. This approach can be extended to the isotopic characterization of elements contained in any chemical species by electrospray mass spectrometry, and appears therefore to be promising for the use this technique by its own for elemental speciation analysis. The implementation of this approach to LC-ESIMS

coupling is of great interest for the comprehensive speciation study of elements in various fields. Such comprehensive speciation is of great concern in applications associated with the nuclear fuel cycle for the development of spent fuel treatment processes, in nuclear toxicology to study the effect of radioelements at the cellular and molecular level and design specific decorporation agents, in geosciences to determine the distribution processes of contaminants chelated to different organic ligands in environmental compartments and in life sciences to better understand the mechanisms underlying the toxicity of metals.

Conflicts of interest

There is no conflict of interest to declare.

Acknowledgements

The authors would like to acknowledge the CEA for its financial support.

References

1 D. M. Templeton, F. Ariese, R. Cornelis, L.-G. Danielsson, H. Muntau, H. P. Van Leeuwen and R. Lobinski, *Pure Appl. Chem.*, 2000, **72**, 1453–1470.
2 D. M. Templeton and H. Fujishiro, *Coord. Chem. Rev.*, 2017, **352**, 424–431.
3 EGADSNF, Paris, France, OECD, NEA/NSC/WPNCS/DOC, 2011, 5.
4 D. Schaumlöffel and A. Tholey, *Anal. Bioanal. Chem.*, 2011, **400**, 1645–1652.
5 S. Miah, S. Fukiage, Z. A. Begum, T. Murakami, A. S. Mashio, I. M. M. Rahman and H. Hasegawa, *J. Chromatogr. A*, 2020, **1630**, 461528.
6 L. Beuvier, C. Bresson, A. Nonell, L. Vio, N. Henry, V. Pichon and F. Chartier, *RSC Adv.*, 2015, **5**, 92858–92868.
7 M. J. Keith-Roach, *Anal. Chim. Acta*, 2010, **678**, 140–148.
8 R. Jirásko and M. Holčapek, *Mass Spectrom. Rev.*, 2011, **30**, 1013–1036.
9 C. Shiea, Y. L. Huang, S. C. Cheng, Y. L. Chen and J. Shiea, *Anal. Chim. Acta*, 2017, **968**, 50–57.
10 M. E. Ketterer and J. P. Guzowski, *Anal. Chem.*, 1996, **68**, 883–887.
11 M. C. B. Moraes, J. G. A. Brito Neto and C. L. do Lago, *J. Anal. At. Spectrom.*, 2001, **16**, 1259–1265.
12 C. Liu, B. Hu, J. Shi, J. Li, X. Zhang and H. Chen, *J. Anal. At. Spectrom.*, 2011, **26**, 2045–2051.
13 J. C. Dubois, G. Retali and J. Cesario, *Int. J. Mass Spectrom. Ion Process.*, 1992, **120**, 163–177.
14 M. Bourgeois, H. Isnard, A. Gourgiotis, G. Stadelmann, C. Gautier, S. Mialle, A. Nonell and F. Chartier, *J. Anal. At. Spectrom.*, 2011, **26**, 1660–1666.
15 J. Kragten, *Analyst*, 1994, **119**, 2161–2165.
16 K. Scheubert, F. Hufsky and S. Böcker, *J. Cheminform*, 2013, **5**, 1–24.
17 J. A. Yergey, *Int. J. Mass spectrom. Ion Physics*, 1983, **52**, 337–349.
18 M. Berglund and M. E. Wieser, *Pure Appl. Chem.*, 2011, **83**, 397–410.
19 J. Meija, T. B. Coplen, M. Berglund, W. A. Brand, P. De Bièvre, M. Gröning, N. E. Holden, J. Irrgeher, R. D. Loss, T. Walczyk and T. Prohaska, *Pure Appl. Chem.*, 2016, **88**, 293–306.